Insulating phases in a two-dimensional electron system of high-mobility Si MOSFET's

A.A. Shashkin, V.T. Dolgopolov, and G.V. Kravchenko
Institute of Solid State Physics, Chernogolovka, 142432 Moscow District, Russia
(Received 23 November 1993)

We have investigated the transport properties of insulating phases in Si MOSFET's at extremely low temperatures. It has been found that insulating phases in the quantum Hall regime behave in a way that is similar to a low-density insulating phase: for all phases we find similar behavior of both the activation energy for the resistance in the linear part of the current-voltage characteristics and the critical electric field corresponding to the onset of nonlinearity. A characteristic length extracted from measurements of the activation energy and critical electric field has been found to diverge near each metal-insulator phase boundary. These results support the localization and reject the Wigner crystal as the origin for any insulating phase. Nonlinear current-voltage characteristics of the insulating phases can be explained by electric-field-induced electron delocalization. We have obtained the critical index for the localization length $s \approx 1$, which is close to the value $s = 1.3$ for classical percolation. We have tested that the effect of temperature can also be treated in terms of delocalization so that the temperature dependence of the width of peaks in the conductivity is explained by the thermal shift of the effective mobility edge of a Landau level. The experimental results point out the existence of the mobility edge in two-dimensional systems in zero magnetic field, in contrast with the predictions of scaling theory.

I. INTRODUCTION

Recently much interest has been paid to the origin of a low-density insulating phase in the two-dimensional (2D) electron gas. At low electron densities the ground state of an ideal 2D electron system is expected to be a Wigner crystal.[1-3] The state of a real 2D electron gas in the presence of potential fluctuations is determined by the relation between the energy of electron-electron interactions and the amplitude of a random potential. It is obvious that in a strong random potential localization of electrons should take place. Results of experimental investigations on Si MOSFET's (Refs. 4 and 5) have been interpreted in terms of Anderson localization at low electron densities. However, some doubts in this interpretation have been expressed in recent works.[6-8] In these experiments strongly nonlinear current-voltage characteristics were observed in the insulating phase: the dependence $V(I)$ is linear below some threshold voltage V_c and saturated at $V > V_c$.[8,9] The resistance corresponding to the linear part of the I-V characteristics reveals an activated temperature dependence. Knowing the values of the threshold voltage and activation energy one obtains a characteristic length that is large compared to the distance between electrons, which excludes single-electron localization and an explanation of nonlinearity in the single-electron model. In some publications[6-8] such behavior was considered to be an indication in favor of the Wigner crystal.

In the 2D case, apart from a low-density insulating phase, there exist insulating phases in the regime of the quantum Hall effect (QHE): at filling factors close to an integer the Fermi level is in a region of localized states. Below the Fermi level there are the extended states of Landau levels capable of carrying a Hall current. (In the case of the Hall bar sample the Hall current is carried also by the extended edge states at the Fermi level.) Because at sufficiently low temperatures the dissipative conductivity σ_{xx} tends to zero, this state is an insulator. Obviously, properties of the insulating phase defined in such a way depend on the number of Landau levels below the Fermi level, i.e., the insulating phase is characterized by the Hall conductivity value. In weak magnetic fields only a zero-Hall-conductivity insulating phase is realized at low electron densities; see Fig. 1. When the Fermi level lies in the extended states of a Landau level

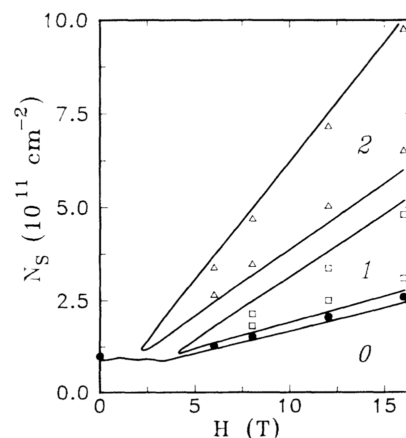

FIG. 1. Metal-insulator phase diagram in the H, N_s plane determined in two ways: (i) at a fixed value of $\sigma_{xx}^{-1} = 500$ kΩ (solid lines) and (ii) at vanishing activation energy (symbols). Digits indicate the Hall conductivity in units e^2/h for different insulating phases.

0163-1829/94/49(20)/14486(10)/$06.00 ©1994 The American Physical Society

the dissipative conductivity is finite and the 2D electron system demonstrates a metallic behavior. Investigations of the metal-insulator phase diagram for the 2D electron gas in Si MOSFET's reveal that in the H, N_s plane each insulating phase is surrounded by the metallic one[10] (Fig. 1). Hence, a transition into the low-density insulating phase occurs only if all the extended states have passed, leaving the Fermi sea, through the Fermi level. These results point out the similarity between all insulating phases characterized by different values of the Hall conductivity. The aim of the present paper is to prove this statement by studying transport properties of the electron system in the insulating phases.

The remainder of the paper is organized as follows. In Sec. II we discuss the possibility of a comparison of transport properties of the insulating phases with different values of σ_{xy}. Section III describes samples and experimental technique. In Sec. IV we report the experimental results on the Hall bar and Corbino samples; these results as well as their relation to the Hall current pinch in the QHE regime and to the scaling behavior of conductivity are discussed in Sec. V. The main results are summarized in Sec. VI.

II. *I-V* CHARACTERISTICS OF INSULATING PHASES

By the properties of insulating phases to be studied we mean nonlinear current-voltage characteristics which define the values of resistance in the linear regime and the critical voltage corresponding to the onset of nonlinearity. As long as the resistance shows an activated temperature dependence one can determine the density of states in an insulating phase by measuring the activation energy as a function of electron density.[11–13] In the present paper we are going to compare the following characteristics of different insulating phases: (i) the density of states at the metal-insulator transition and (ii) the behavior of the critical voltage in the vicinity of metal-insulator phase boundary.

For measurements of *I-V* characteristics the use of Corbino samples is convenient. Indeed, in quantizing magnetic fields there are two current channels in a sample: the dissipative channel at the Fermi level and the dissipationless one through the extended states of Landau levels. In the Corbino samples these current channels are disconnected because the dissipationless Hall current does not contribute to the radial one proportional to σ_{xx}. Hence, measuring the dependence of the potential drop between contacts on radial current through the sample we obtain *I-V* characteristics for any insulating phase. Below we discuss the Hall bar geometry in view of *I-V* characteristics.

In contrast to the case of Corbino geometry, in the Hall bar sample the current channels are connected with each other owing to the existence of edge channels. When the Fermi level lies in the extended states of a Landau level, electrons are backscattered between the opposite edge channels by tunneling between different Landau levels at the sample edges and diffusing through the upper Landau level in the bulk. The transverse (backscattering) current has to be compensated by the drift motion of electrons in Landau levels that gives rise to the longitudinal potential drop associated with ρ_{xx}.[14] If the tunnel resistance determined by a tunneling rate between Landau levels is not vanishingly small, the upper Landau level will be decoupled, which results in nonlocal effects.[15,16] In this case the longitudinal resistance depends also on the tunnel resistance and contact properties.[14,17–20] On our Hall bar samples the nonlocal effects were not significant because values of σ_{xx} calculated from the resistances measured were close to those obtained for Corbino samples.

Let us now consider the case of filling factors close to integer, i.e., the QHE regime. It is well known that at some value of the dissipationless bias current the resistivity ρ_{xx} rapidly grows and the QHE breaks down. This phenomenon has been studied for a long time; however, it was impossible to distinguish unambiguously the breakdown mechanism. A few possible mechanisms for the breakdown, which include the bulk and edge ones, have been proposed over the years: (a) thermal instability, whereby the rate of gain of energy by the electrons exceeds their ability to relax by transfering energy to lattice modes[21,22] (heating of the electrons eventually leads to inter-Landau level transitions); (b) spontaneous emission of phonons when the electron drift velocity exceeds the velocity of sound in the substrate material;[23,24] (c) injection of nonequilibrium electrons from the current contact;[25] (d) quasielastic inter-Landau level transitions accompanied by acoustic phonon emission at large values of the Hall field;[26–28] (e) change of the mobility threshold in the Hall electric field;[29] (f) interedge state tunneling and backscattering;[30] and (g) successive breakdown of small localized inhomogeneous regions within the device[31] due to any of the above processes.

Experiments utilizing a photoresistance imaging technique for macroscopic samples of $Al_xGa_{1-x}As/GaAs$ heterostructures[32] have been performed recently. As shown in that paper, the behavior of the longitudinal resistance and 2D images makes it possible to distinguish three stages in development of the breakdown: (i) the initial rise of the longitudinal resistance is due to a change with the Hall electric field of the percolation threshold leading to electron backscattering between the edges; (ii) at higher bias currents a strong response from the edges is observed in 2D images, in agreement with the edge state model; and (iii) on increasing the bias current further, electron heating effects start to prevail. Thus, all the mechanisms mentioned above are classified in Ref. 32 and the conclusion is drawn that the QHE breakdown really occurs in the bulk of the sample owing to the electron delocalization in an electric field which leads, for the Hall bar sample, to an abrupt increase of backscattering current flowing at the Fermi level between opposite edge channels. Because the backscattering current is identical to the radial one in a Corbino sample, both of the sample geometries are equivalent in the sense of QHE breakdown. In a similar way to Corbino geometry, in the case of the Hall bar sample *I-V* characteristics of an insulating phase in the QHE regime is the Hall potential difference as a function of backscattering current. We

note that as long as $\sigma_{xx} \ll \sigma_{xy}$, the quantized value of σ_{xy} is a factor of proportionality between the bias current I_{sd} and the Hall voltage U as well as between the backscattering current I and the longitudinal potential drop U_{xx}. Since in the experiment we measure dependence $U_{xx}(I_{sd})$, it is necessary to calculate $I = \sigma_{xy} U_{xx}$ and $U = \sigma_{xy}^{-1} I_{sd}$ for comparison with the results for the low-density insulating phase. Henceforth the dependence $U(I)$ will be referred to as I-V characteristics of the insulating phase in the QHE regime.

Finally, in the case of a low-density insulating phase there is only a dissipative current channel in the sample. For this phase the inequality $\sigma_{xx} \gg \sigma_{xy}$ is valid;[33–36] therefore I-V characteristics are the longitudinal voltage U_{xx} as a function of bias current I_{sd}.

In the present paper we show that in Si MOSFET's I-V characteristics of the low-density insulating phase behave in a way that is similar to those of insulating phases in the QHE regime. (The resemblance of I-V characteristics of the low-density insulating phase in $Al_xGa_{1-x}As/GaAs$ heterostructures to the QHE breakdown characteristics was observed, according to Ref. 37, in the high-voltage limit.) Two main consequences follow from the experimental observations: (i) localization of electrons is the origin of the low-density insulating phase and (ii) the mechanism of nonlinearity observed for this phase is the same as that of the QHE breakdown and due to the electron delocalization in an electric field, at least near the metal-insulator boundary.

III. EXPERIMENTAL TECHNIQUES

From the above discussions one can see that I-V characteristics for all the insulating phases are directly measured on Corbino samples. However, in order to realize such measurements the contact resistances should be small, which is not the case on our Si MOSFET's at low electron densities.

The main part of our measurements was made on high-mobility ($\mu_{\text{peak}} \sim 3\times10^4$ cm^2/V s at $T = 1.3$ K) Hall bar Si MOSFET's in a range of low electron densities (down to $\sim 8 \times 10^{10}$ cm^{-2}) at temperatures down to ~ 25 mK. The two samples had dimensions 0.25×2.5 mm^2 with distances between the nearest potential probes 0.625 mm. The SiO_2 layer thickness was equal to $\sim$ 1800 Å.[38] In magnetic fields of up to 16 T dependences of the longitudinal voltage on the bias current were recorded in the low-density insulating phase and in the regions of QHE plateaus with filling factors 1 and 2. These experimental results were obtained by a four-terminal dc technique using an electrometer as high-input-resistance amplifier.

I-V characteristics for all insulating phases at a minimum temperature when the nonlinearities are most pronounced were used to determine the threshold voltage (Fig. 2). The temperature dependence of resistance of the linear part of I-V characteristics gives the value of activation energy E_a. We investigated the behavior of the threshold voltage and activation energy as a function of the electron density N_s at a fixed value of magnetic field. Regions of N_s were chosen so that the Fermi level was close to a mobility edge.

Part of the measurements on the Hall bar samples at relatively high electron densities was carried out by a standard lock-in technique at a frequency of 10 Hz. The value of the current through the sample was 1 nA and corresponded to the linear regime. In these experiments we investigated the scaling behavior of conductivity in order to find out its relation to the results obtained for an insulating phase.

In the case of insulating phases with nonzero σ_{xy} the dependence of threshold voltage on magnetic field at fixed N_s can also be measured in the experiments on charge transfer in Corbino samples. This method to determine breakdown voltages can be used even at high contact resistances. We briefly outline the experimental technique, which is described in detail in Refs. 39 and 40. A magnetic field H was applied normal to the plane of 2D electron gas and changed linearly with time. The induced azimuthal electric field causes charge transfer below the Fermi level between the contacts in a similar manner to Laughlin's gedanken experiment.[41] At min-

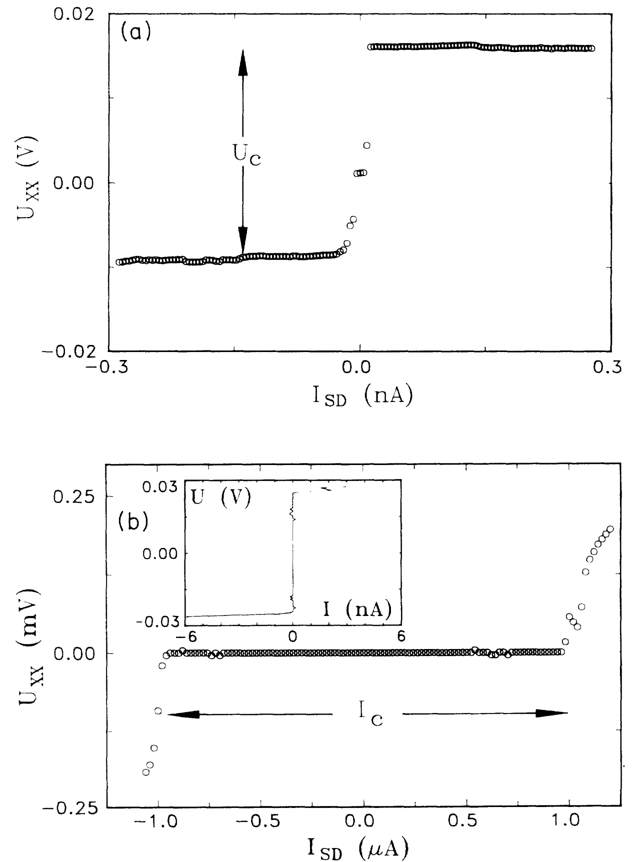

FIG. 2. Current-voltage characteristics at a minimum temperature: (a) for the low-density insulating phase ($H = 12$ T and $N_s = 1.74 \times 10^{11}$ cm^{-2}) and (b) for the insulating phase with $\sigma_{xy}h/e^2 = 1$ ($H = 12$ T and $N_s = 2.83 \times 10^{11}$ cm^{-2}). In (b) we measure the breakdown dependence $U_{xx}(I_{sd})$ and then convert it into I-V characteristics $U(I)$ (inset) as described in the text of the paper.

ima of σ_{xx} the back charge transfer was negligible during the experiment at sufficiently low temperatures and low enough potential difference due to the buildup of charges in the contacts. In the absence of back charge transfer the potential difference is inversely proportional to the input capacitance of an electrometer and proportional to the increment of magnetic field. As was found in Ref. 42, the linear rise of voltage with magnetic field changes by a drop along the ultimate curve corresponding to the QHE breakdown. At sufficiently small values of the input capacitance the entire experimental dependence of the potential difference on magnetic field becomes independent of the capacitance value and tends to the ultimate curve corresponding to the breakdown voltage.

To study the charge transfer we used Si MOSFET's of the Corbino geometry with the following parameters: internal diameter $2r_1 = 225$ μm, external diameter $2r_2 = 675$ μm, SiO_2 was 1300 Å thick, and mobility at maximum $\mu \sim 2 \times 10^4$ cm^2/V s at $T = 1.3$ K.

IV. RESULTS

The metal-insulator phase diagram in the H, N_s plane is presented in Fig. 1. The position of phase boundaries was determined in two ways: first, assuming that at vanishing temperature the metal-insulator transition occurs at a fixed value of $\sigma_{xx}^{-1} = 500$ kΩ;[10] and second, by means of measurements of the activation energy in an insulating phase since it tends to zero when the phase boundary is approached.[9] The values of σ_{xx} on the boundary corresponding to zero activation energy proved to be $\sigma_{xx}^{-1} \simeq 500$ kΩ for the insulating phases with $\sigma_{xy}h/e^2 = 1, 2$ and $\sigma_{xx}^{-1} \simeq 100$ kΩ for the low-density phase. However, the discrepancy between the results of two methods is small, see Fig. 1. As will be discussed below, the latter method is correct.

It is very important that the neighboring insulating phases are separated by metallic strips, i.e., there is no insulator-insulator transition. In other words, in the region of low electron densities *there exist two transition points on the interval of monotonic growth of* ρ_{xx} *from zero to infinity* since both $\rho_{xx} \to 0$ and $\rho_{xx} \to \infty$ correspond to $\sigma_{xx} \to 0$. We emphasize that our experimental phase diagram contradicts the global phase diagram introduced in Ref. 43, because the former allows a transition, e.g., from the phase with $\sigma_{xy}h/e^2 = 2$ to the low-density insulating phase.

Figures 2(a) and 2(b) demonstrate the typical current-voltage characteristics for the insulating phases with $\sigma_{xy}h/e^2 = 0$ and 1, respectively. One can see from Fig. 2(a) that at a minimum temperature the dependence $U_{xx}(I_{sd})$ is very close to the steplike function due to the high resistance in the linear interval. (The longitudinal voltage is normalized everywhere in the paper by the aspect ratio which is equal to 2.5 for our Hall bar samples.) Figure 2(b) shows $U_{xx}(I_{sd})$ corresponding to the QHE breakdown. The result of the conversion of the breakdown curve into I-V characteristics, as described above, is displayed in the inset. It is clearly seen that I-V characteristics of different insulating phases are very similar. The critical voltage can be easily determined from these dependences as half of the step height.

Measuring the critical voltage at various N_s at a fixed magnetic field we find that near each mobility edge it obeys, within experimental uncertainty, the following law:

$$U_c/2 = \alpha(N_s - N_c)^2, \tag{1}$$

where N_c corresponds to electron density at the mobility edge (Fig. 3). As seen from Fig. 3, coefficients of the proportionality are of the same order of magnitude so that all the insulating phases behave in a similar way. In the metallic phase in between the neighboring values of N_c we observe linear I-V characteristics in the range of currents used.

The behavior of the critical voltage is confirmed in the experiments on charge transfer in Corbino samples. In this case the part of experimental dependence of the potential difference U between contacts on the magnetic field corresponds to the ultimate curve (Fig. 4). Figure 4 demonstrates that the ultimate curve obeys the same power law in the vicinity of mobility edge. Thus the critical voltage increases as square of the distance from the phase boundary in the H, N_s plane. This fact is found for all insulating phases investigated.

The activated temperature dependence of the resistance in the linear interval of I-V characteristics changes at low temperatures to the variable range hopping one (Fig. 5). Measurements of the activation energy at different electron densities when the Fermi level is close to the mobility edge enable us to determine the density of states D at the mobility edge. Indeed, E_a is proportional to a change in N_s (Fig. 6) so that $D = \partial N_s/\partial E_F = | \partial N_s/\partial E_a |$. One can see from Fig. 6 that both the critical voltage and activation energy come to zero at the same electron density N_c, as was expected. This fact was checked at all the points depicted in Fig. 1. Moreover, extrapolation of the linear temperature dependence of the width of peaks in ρ_{xx} to a zero temperature (Fig. 7) gives the value of N_c which is consistent with that obtained

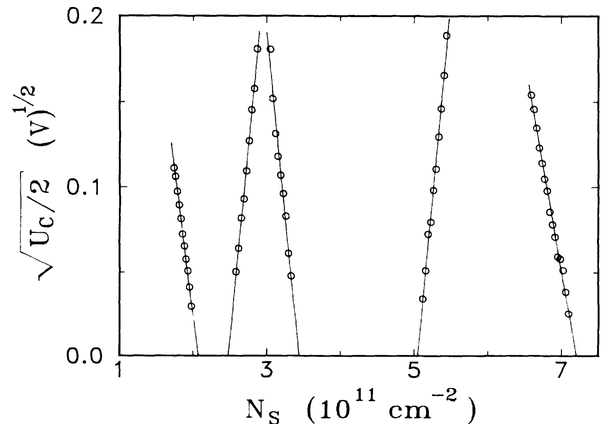

FIG. 3. Square root out of the critical voltage against electron density at the phase boundaries corresponding to $\sigma_{xy}h/e^2 = 0, 1, 2$ in a magnetic field $H = 12$ T.

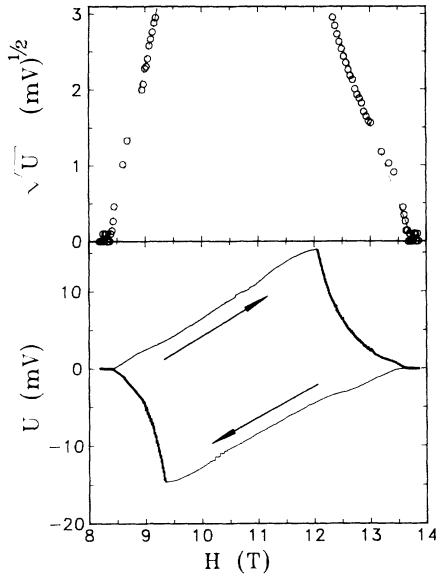

FIG. 4. Measurements of the charge transferred between the contacts of the Corbino sample when sweeping the magnetic field around the filling factor $\nu = 2$. Bottom: potential difference between the sample contacts as a function of magnetic field. A part of the ultimate curve is shown by bold lines. Arrows indicate the sweep direction of H. Top: square root of the absolute value of voltage on the ultimate curve.

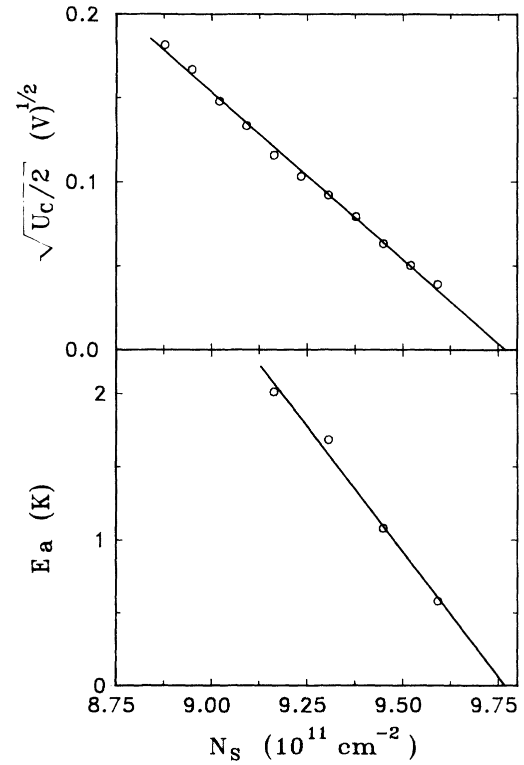

FIG. 6. Behavior of the critical voltage and the activation energy near the phase boundary. $H = 16$ T.

from measurements of the activation energy. Hence we can introduce the correct definition of the metal-insulator transition point as a point of vanishing activation energy.

It is interesting to investigate the behavior of α and D on the phase boundaries. With increasing magnetic field the coefficient α on a given boundary tends to decrease (Fig. 8) while the density of states reveals the opposite tendency. From our experimental results it seems difficult to find some regular behavior of α at different phase boundaries at a fixed magnetic field. Anyway, there is nothing special for any insulating phase so that the experimental results prove the similarity of all insulating phases including the low-density phase.

V. DISCUSSION

The results obtained show that in all insulating phases the electron system has very similar properties. As is known, in Si MOSFET's there exist, due to the spin and valley splitting, four quantum levels having the same

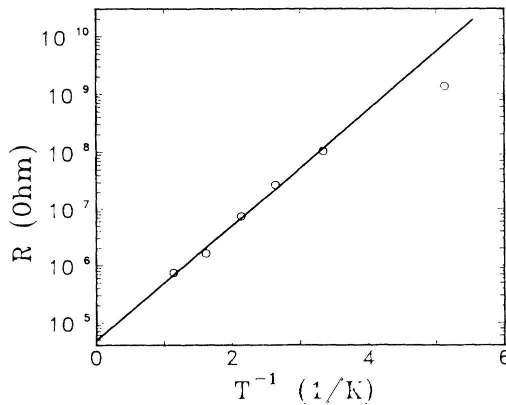

FIG. 5. Arrhenius plot of resistance of the linear interval of I-V characteristics. $H = 16$ T and $N_s = 2.17 \times 10^{11}$ cm^{-2}. The deviation at low temperatures points out the change of the conductivity mechanism.

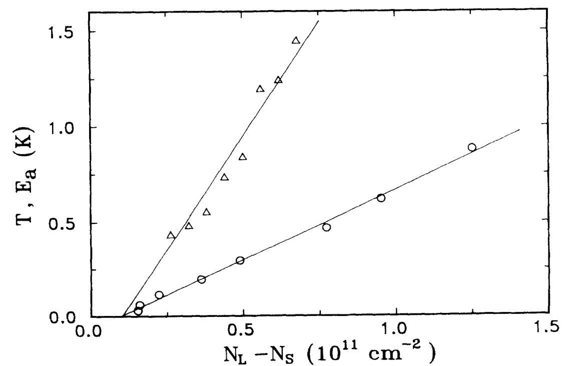

FIG. 7. Temperature dependence of the width $N_L - N_s$ of a peak in ρ_{xx} (determined at half of the peak height) on another Hall bar sample (circles). We counted the peak width from N_L in order to compare this dependence with the behavior of the activation energy (triangles). $H = 14$ T. The peak corresponds to a filling factor $\nu = 2.5$.

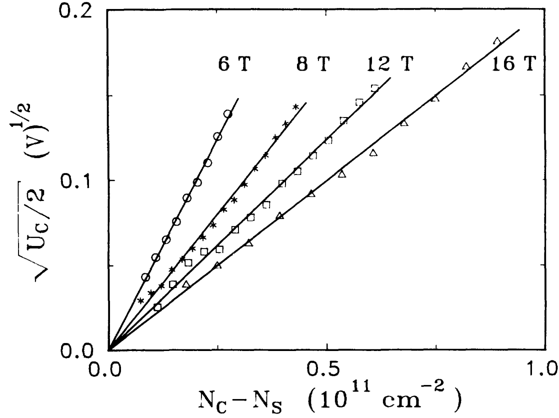

FIG. 8. Square root of the critical voltage as a function of deviation $N_c - N_s$ from the upper boundary of the insulating phase with $\sigma_{xy}h/e^2 = 2$ at different magnetic fields.

wave functions. Electrons of the upper Landau level should occupy the potential minima in the same succession order as those of the lower Landau levels if the screening of random potential by electrons of totally occupied levels is negligible.

In order to analyze nonlinear I-V characteristics of the low-density insulating phase the following argumentation has been used:[6–8] the localization length of electrons can be evaluated from the relation

$$| E_F - E_c | = eLF_c = eL(\alpha D^2/d)(E_F - E_c)^2 = eL\beta(E_F - E_c)^2, \quad (2)$$

where $F_c = U_c/2d$ is the critical electric field, d is a width of sample, and e is an electron charge. By using the typical parameters $E_a = | E_F - E_c | = 1$ K and $F_c = 0.1$ V/cm one can obtain the localization length $L \approx 8$ μm. This evaluation shows that nonlinear behavior cannot be explained by the electric-field-induced breakdown of individual electron localization,[9] because the localization length is large compared to the distance between electrons. In a number of experimental works[6–8] this fact has been considered as evidence of a Wigner crystal. In this case it would be reasonable to associate the length L with the size of a Wigner crystallite. However, any estimation of the crystallite size leads, in agreement with our results, to the divergency of L near the transition point, which seems dubious. As was shown in Ref. 10, the metal-insulator phase diagram points out the similarity between the low-density insulating phase and insulating phases in the QHE regime because an insulator-insulator transition is absent. The results of the present paper prove the similarity of all insulating phases, thereby completely rejecting the Wigner crystal as the possible origin of the insulating phase.

In our opinion, the existence of a large characteristic length is in favor of the percolation picture in which L should be the cluster dimension (or the localization length). Indeed, at sufficiently low temperatures the conduction in the insulating phase is due to variable range hopping (Fig. 5) while in a cluster the electron system is metallic. This implies that at electric fields less than F_c the cluster at $E = E_F$ is equipotential, i.e., the minimum energy separation between the mobility edge and cluster decreases as compared to $| E_F - E_c |$. At the threshold value of the electric field given by Eq. (2), where L is the radius of cluster at $E = E_F$, this energy separation equals zero (in other words, the electrons reach the mobility edge), which gives rise to an abrupt increase of conduction in agreement with experiment. It is clear that at higher temperatures the nonlinearity will be smeared out leading to smooth current-voltage characteristics. (By the electron delocalization in an electric field we can also explain the peculiarities in charge transfer observed in the experiments on Corbino samples with a circular gate for creating inhomogeneous distributions of electron density.[44])

In such a picture one should expect the parameter β to be weakly dependent on magnetic field. This is really the case; see Table I. Moreover, the values of β for different phase boundaries are approximately the same. Looking at Table I it is difficult to find some regular dependence of the coefficient β since the accuracy of determination of D is not high. One can only state that such a dependence should be weak, if β changes at all. The relative dispersion of β is equal to 30% while that of α is 80%.

We note that Eq. (2) is consistent with the known expression for cluster dimension in the vicinity of mobility edge

$$L(E) \propto | E - E_c |^{-s} . \quad (3)$$

In our case the critical index $s \approx 1$, which is in agreement with the theoretical value in classical percolation problem $s = 1.3$ (Ref. 45) within experimental uncertainty. So, electric-field-induced electron delocalization in the classical percolation picture is capable of explain-

TABLE I. Density of states D and coefficients α, β on a given phase boundary at different magnetic fields. The phase boundaries are denoted in the following way: 0 for the low-density insulating phase, $1l$ and $1u$ for lower and upper boundaries for the insulating phase with $\sigma_{xy}h/e^2 = 1$, etc.

H (T)		0	6	8	12	16
α (10^{-22} cm^4 V)	0	0.21	0.35	0.22	0.11	0.071
	$1l$			0.69	0.20	0.11
	$1u$			0.49	0.18	0.092
	$2l$		0.60	0.51	0.21	0.12
	$2u$		0.25	0.11	0.061	0.040
D (10^{14} cm^{-2} eV^{-1})	0	1.50	1.14	1.15	1.64	2.20
	$1l$			0.88	2.01	1.79
	$1u$			1.12	1.53	2.07
	$2l$		0.88	0.87	1.26	1.53
	$2u$		1.00	1.96	2.31	3.37
β (V cm^{-1} K^{-2})	0	0.14	0.13	0.09	0.09	0.10
	$1l$			0.16	0.24	0.10
	$1u$			0.18	0.12	0.11
	$2l$		0.14	0.11	0.10	0.08
	$2u$		0.07	0.12	0.10	0.13

ing the experimental observations. However, in order to substantiate our model, we have to answer, first of all, the following questions: (i) How can the macroscopic change in electron density caused by an electric field (in particular, the Hall current pinch[46,47]) influence the shape of I-V characteristics? (ii) What is the relationship between the results obtained and the scaling behavior of conductivity?

A. Hall current pinch

Under QHE conditions one can distinguish the two regimes of the screening of external electric field by a 2D electron system: either the thermodynamical equilibrium is available or absent. In the latter case the screening charges do not enter the bulk of the 2D layer within the characteristic time of experiment so that the screening is realized just by charges at the sample edges. An example is experiments with the nonequilibrium populations of different edge channels (e.g., Refs. 48–50) and, on the other hand, the case of sufficiently small σ_{xx}, in particular, the screening by an ideal electron system.[51] In our experiments we dealt with the equilibrium regime owing to the proximity of E_F to mobility edge: I-V characteristics were the same when we cooled the sample down from the equilibrium state either turning the bias current on or keeping $I_{sd} = 0$. Since in the equilibrium regime there exists the Hall current pinch[46,47] we have to discuss this effect.

At large enough Hall potential difference the local change of electron density may result in an appreciable variation of the conductivity σ_{xx} over a sample because σ_{xx} depends on filling factor ν. As a result, the Hall current flows in the narrow channel corresponding to a minimum σ_{xx}. The stronger the dependence of dissipative conductivity on filling factor, the smaller the width of the current channel. The latter decreases also with increasing Hall voltage. The Hall current pinch was experimentally detected in the QHE regime at relatively high temperatures when activation transport dominates, leading to the exponential dependence of σ_{xx} on the filling factor.

In the case of the low-density insulating phase the large longitudinal voltage results in similar nonlinear effects: the voltage drops at the place where σ_{xx} is minimal, i.e., the effective length of the sample decreases. Hence the change of electron density can be, in principle, the origin for nonlinear I-V characteristics. However, this is really not the case because of the following reasons. (i) The typical change in N_s due to potential difference in the plane of the 2D electron gas is small compared with $| N_s - N_c |$. As a result, I-V characteristics are mostly symmetrical, except for the maximum $| N_s - N_c |$, where the asymmetry does appear, in the first turn, for the low-density insulating phase since the aspect ratio is more than unity (Fig. 2). (ii) At lowest temperatures the variable range hopping conductivity becomes dominant; therefore the dependence of σ_{xx} on the filling factor should be weak. (iii) Subject to the validity of the nonlinear mechanism in question, we obtain a nonphysical behavior of the density of states determined from nonlinear characteristics at relatively high temperatures.[52] This points out the existence of another mechanism of nonlinearity. (iv) Also, it is difficult to explain the threshold behavior of I-V characteristics at lower temperatures.

B. Scaling behavior of conductivity

As was found in a number of experiments (see, e.g., Refs. 53–58), the width of peaks in σ_{xx} (or ρ_{xx}) follows a power law

$$\Delta\nu \propto T^{\kappa}, \tag{4}$$

where $\kappa \simeq 0.4$ in the case of low-mobility heterostructures and $\kappa \approx 1$ for Si MOSFET's. The conventional explanation of the scaling dependence (4) is based on the existence of a temperature-dependent phase-coherence length L_Φ that determines the position of the effective mobility edge $E_{\rm eff}$.[59,60] If the localization length L given by Eq. (3) is more than L_Φ, these electron states should be effectively delocalized. Hence $E_{\rm eff}$ is connected with temperature via some L_Φ. We note that this consideration implies the Anderson localization of electrons which occurs in a weak short-range random potential: the electron wave functions are overlapped so that each inelastic process (with the typical energy about kT) should delocalize electrons. In the case of long-range or strong random potential the percolation picture is valid, and one can give the following explanation of temperature dependence of the peak width.

We argue that in the percolation picture the effect of temperature is similar to that of the electric field discussed above. Indeed, the conduction between clusters due to electron thermoactivation to the mobility edge is of the order of maximum σ_{xx} when the activation energy $E_a \sim kT$. Hence we can introduce the effective mobility edge $E_{\rm eff}$ so that

$$| E_{\rm eff} - E_c | = \gamma kT. \tag{5}$$

Here γ is a numerical coefficient of the order of unity. Assuming that near the mobility edge E_c the density of states is constant, we conclude that a change of the width of the σ_{xx} peak should be proportional to temperature. Such a situation takes place in Si MOSFET's; see Fig. 7. The width of peak $| N_L - N_s |$ (N_L pertains to the center E_L of a Landau level) gives the value of N_s corresponding to the effective mobility edge $E_{\rm eff}$. Since the position of $E_{\rm eff}$ can be determined by measuring the activation energy (Fig. 7), we find $\gamma \approx 3$. As seen from the figure, both the dependences run to the same point $N_L - N_c \neq 0$, which contradicts the scaling relation (4). This means that the mobility edge E_c does not coincide with the center of the Landau level E_L. In agreement with Ref. 56, we believe that the position of E_c is determined by the sample size so that in the sample of finite dimensions the region of extended states in the Landau level is finite. Using the data from Fig. 7 we can roughly estimate $E_L - E_c < (N_L - N_c)/D \approx 0.2$ K. The difference is small;

therefore our results are in agreement with the concept of the divergency of the localization length at the center of a Landau level in the case of infinite sample

$$L(E) \propto | E - E_L |^{-s}, \quad (6)$$

where s is close to the theoretical prediction $s = 1.3$. Knowing the value of β, we obtain by means of Eq. (6) another evaluation $| E_L - E_c | \approx 0.1$ K, which seems reasonable since the temperature dependence of the width of peaks in ρ_{xx} is observed down to minimum temperatures.

We suppose that these arguments also hold for heterostructures. In this case $| E_L - E_c |$ is probably less than in Si MOSFET's and the assumption about the density of states weakly varying near E_c may be wrong. As a result, the exponent κ can be less than unity. There is also another reason for decreasing κ: one cannot use Eq. (4) since at $T \to 0$ the width $\Delta\nu$ is finite due to the finite dimensions of sample. If we do use it we will artificially reduce κ. For instance, in Ref. 54 the value of κ has been found to approach unity as the temperature increases. When replotted in the linear scale the data $\Delta\nu(T)$ taken from Ref. 54 behaves in a way that is similar to the case of Si MOSFET's (Fig. 7).

Numerical calculations of the critical index s provide $s \approx 2$ (e.g., Refs. 61–63). We do not think that a comparison of this value with our experimental results makes sense because the calculations are made for submicrometer samples while the measurements were performed on macroscopic samples. In the first case $| E_L - E_c |$ is expected to be large so that E_c lies in the region where the behavior of $L(E)$ can be different.

It seems evident that the coefficient β should depend on the parameters of a random potential. The above discussions enable us to make the following suggestion: *the higher the quality of sample, the more* β, so that for an ideal system the dependence (6), which is valid only in the vicinity of E_L tends to a δ function. This implies that far from E_L the localization length should change with an energy stronger as compared to Eq. (6). If this suggestion is true, then in order to reach the vicinity of E_L where the relation (6) is valid, either the low-quality samples should have very large dimensions or the small samples should be of very high quality. In such a way we can account for the dependence of the minimum peak width on the sample dimensions (see Ref. 56) that yields $s \approx 2$: the samples used in Ref. 56 are an order of magnitude less than ours. Hence the characteristic energies corresponding to the smaller samples may be too far from E_L where the expression (6) is not applicable.

From Table I it follows that the behavior of the localization length near the mobility edge hardly depends on the value of magnetic field. This implies that in the absence of a magnetic field there exists a finite mobility edge separating the 2D metallic band from the tail of the localized electron states (see, e.g., Ref. 64). In other words, the measurements of the localization length along with the study of the phase diagram (see Fig. 1 and Ref. 10) prove the existence of the mobility edge in a 2D system in a zero magnetic field.[65] This is in contradiction to scaling theory.[66]

VI. CONCLUSION

In summary, we have investigated nonlinear current-voltage characteristics in the case of Si MOSFET's for a low-density insulating phase as well as for insulating phases in the QHE regime and found that for all the insulating phases these characteristics behave in a similar way. This fact contradicts the hypothesis about the formation of a Wigner crystal as the origin for the low-density insulating phase and supports the localization picture. Then, the nonlinearities on I-V characteristics find their natural explanation as electric-field-induced delocalization of the electron states which is also the reason for the QHE breakdown, as has been shown in a recent paper.[32] The measurements of the critical electric field and activation energy enable us to determine the localization length that has been found to diverge near each metal-insulator phase boundary with the critical index close to the theoretical value $s = 1.3$ for classical percolation. The larger values of s obtained elsewhere can be due to the smaller dimensions of samples used. The behavior of the metal-insulator phase diagram and the localization length proves the existence of the mobility edge in a 2D system in the absence of a magnetic field, in contrast to the predictions of scaling theory. In zero and weak magnetic fields the position of the mobility edge is determined by the bottom of the 2D electron band. As the magnetic field increases, the Landau levels enter the 2D electron band giving rise to the oscillations of the lower phase boundary,[10] so that in the case of quantizing magnetic fields each Landau level corresponds to the region of extended states due to the finite dimensions of sample. We have shown that in the temperature dependence of the width of the peaks in conductivity the role of temperature is similar to that of the electric field: this effect can be explained by the thermal shift of the effective mobility edge in a Landau level, which is confirmed by the analysis of the data from previous works.

ACKNOWLEDGMENTS

We are grateful to Dr. D.V. Shovkun and Dr. W. Hansen for fruitful discussions of the paper. This work was supported by Volkswagenstiftung under Grant No. I/68553 and, in part, by Grant No. 93-02-2304 from the Russian Foundation for Basic Research and by the Programme "Nanostructures."

[1] Y.E. Lozovik and V.I. Yudson, Pis'ma Zh. Eksp. Teor. Fiz. **22**, 26 (1975) [JETP Lett. **22**, 11 (1975)].
[2] M. Tsukada, J. Phys. Soc. Jpn. **42**, 391 (1977).
[3] P.K. Lam and S.M. Girvin, Phys. Rev. B **30**, 473 (1984).
[4] S. Kawaji and J. Wakabayashi, Solid State Commun. **22**, 87 (1977).
[5] M. Pepper, Philos. Mag. **37**, 83 (1978).
[6] S.V. Kravchenko, J.A.A.J. Perenboom, and V.M. Pudalov, Phys. Rev. B **44**, 13 513 (1991).
[7] S.V. Kravchenko, V.M. Pudalov, J.W. Campbell, and M. D'Iorio, Pis'ma Zh. Eksp. Teor. Fiz. **54**, 528 (1991) [JETP Lett. **54**, 532 (1991)].
[8] V.M. Pudalov, M. D'Iorio, S.V. Kravchenko, and J.W. Campbell, Phys. Rev. Lett. **70**, 1866 (1993).
[9] V.T. Dolgopolov, G.V. Kravchenko, A.A. Shashkin, and S.V. Kravchenko, Phys. Rev. B **46**, 13 303 (1992).
[10] A.A. Shashkin, G.V. Kravchenko, and V.T. Dolgopolov, Pis'ma Zh. Eksp. Teor. Fiz. **58**, 215 (1993) [JETP Lett. **58**, 220 (1993)].
[11] C.J. Adkins, S. Pollitt, and M. Pepper, J. Phys. C **37**, 343 (1976).
[12] E. Stahl, D. Weiss, G. Weimann, K. von Klitzing, and K. Ploog, J. Phys. C **18**, L783 (1985).
[13] M.G. Gavrilov and I.V. Kukushkin, Pis'ma Zh. Eksp. Teor. Fiz. **43**, 79 (1986) [JETP Lett. **43**, 103 (1986)].
[14] V.T. Dolgopolov, G.V. Kravchenko, and A.A. Shashkin, Solid State Commun. **78**, 999 (1991).
[15] B.E. Kane, D.C. Tsui, and G. Weimann, Phys. Rev. Lett. **59**, 1353 (1987); R.J. Haug and K. von Klitzing, Europhys. Lett. **10**, 489 (1989).
[16] P.L. McEuen, A. Szafer, C.A. Richter, B.W. Alphenaar, J.K. Jain, A.D. Stone, R.G. Wheeler, and R.N. Sacks, Phys. Rev. Lett. **64**, 2062 (1990).
[17] S.I. Dorozhkin, V.T. Dolgopolov, G.V. Kravchenko, A.A. Shashkin, and K. von Klitzing, Helv. Phys. Acta **65**, 341 (1992).
[18] S. Komiyama and H. Nii, Physica B **184**, 7 (1993).
[19] P. Svoboda, P. Streda, G. Nachtwei, A. Jaeger, M. Cukr, and M. Laznicka, Phys. Rev. B **45**, 8763 (1992).
[20] C.A. Richter, R.G. Wheeler, and R.N. Sacks (unpublished).
[21] G. Ebert, K. von Klitzing, K. Ploog, and G. Weimann, J. Phys. C **16**, 5441 (1983).
[22] S. Komiyama, T. Takamasu, S. Hiyamizu, and S. Sasa, Solid State Commun. **54**, 479 (1985).
[23] P. Streda and K. von Klitzing, J. Phys. C **17**, L483 (1984).
[24] K. Yoshihiro, J. Kinoshita, K. Inagaki, C. Yamanouchi, Y. Murayama, T. Endo, M. Koyanagi, J. Wakabayashi, and S. Kawaji, Surf. Sci. **170**, 193 (1986).
[25] P.C. van Son, G.H. Kruithof, and T.M. Klapwijk, Phys. Rev. B **42**, 11 267 (1990).
[26] O. Heinonen, P.L. Taylor, and S.M. Girvin, Phys. Rev. B **30**, 3016 (1984).
[27] L. Eaves and F.W. Sheard, Semicond. Sci. Technol. **1**, 346 (1986).
[28] F. Kuchar, G. Bauer, G. Weimann, and H. Burkhard, Surf. Sci. **142**, 196 (1984).
[29] S.A. Trugman, Phys. Rev. B **27**, 7539 (1983).
[30] A.J. Kent, D.J. McKitterick, L.J. Challis, P. Hawker, C.J. Mellor, and M. Henini, Phys. Rev. Lett. **69**, 1684 (1992).
[31] M.E. Cage, R.F. Dziuba, B.F. Field, E.R. Williams, S.M. Girvin, A.C. Gossard, D.C. Tsui, and R.J. Wagner, Phys. Rev. Lett. **51**, 1374 (1983).
[32] A.A. Shashkin, A.J. Kent, P.A. Harrison, L. Eaves, and M. Henini, Phys. Rev. B **49**, 5379 (1994).
[33] V.T. Dolgopolov, G.V. Kravchenko, A.A. Shashkin, and S.V. Kravchenko, Pis'ma Zh. Eksp. Teor. Fiz. **55**, 701 (1992) [JETP Lett. **55**, 733 (1992)].
[34] S.I. Dorozhkin, A.A. Shashkin, G.V. Kravchenko, V.T. Dolgopolov, R.J. Haug, K. von Klitzing, and K. Ploog, Pis'ma Zh. Eksp. Teor. Fiz. **57**, 55 (1993) [JETP Lett. **57**, 58 (1993)].
[35] T. Sajoto, Y.P. Li, L.W. Engel, D.C. Tsui, and M. Shayegan, Phys. Rev. Lett. **70**, 2321 (1993).
[36] K.I. Wysokinski and W. Brenig, Z. Phys. B **54**, 11 (1983).
[37] H.W. Jiang, H.L. Stormer, D.C. Tsui, L.N. Pfeiffer, and K.W. West, Phys. Rev. B **44**, 8107 (1991).
[38] M.A. Vernikov, L.M. Pazinich, V.M. Pudalov, and S.G. Semenchinskii, Elektron. Tekh. **6**, 27 (1985).
[39] V.T. Dolgopolov, N.B. Zhitenev, and A.A. Shashkin, Pis'ma Zh. Eksp. Teor. Fiz. **52**, 826 (1990) [JETP Lett. **52**, 196 (1990)].
[40] V.T. Dolgopolov, N.B. Zhitenev, and A.A. Shashkin, Europhys. Lett. **14**, 255 (1991).
[41] R.B. Laughlin, Phys. Rev. B **23**, 5632 (1981).
[42] V.T. Dolgopolov, A.A. Shashkin, N.B. Zhitenev, S.I. Dorozhkin, and K. von Klitzing, Phys. Rev. B **46**, 12 560 (1992).
[43] S. Kivelson, D.-H. Lee, and S.-C. Zhang, Phys. Rev. B **46**, 2223 (1992).
[44] V.T. Dolgopolov, A.A. Shashkin, G.V. Kravchenko, S.I. Dorozhkin, and K. von Klitzing, Phys. Rev. B **48**, 8480 (1993).
[45] B.I. Shklovskii and A.L. Efros, *Electronic Properties of Doped Semiconductors* (Springer, New York, 1984).
[46] A.A. Shashkin, V.T. Dolgopolov, and S.I. Dorozhkin, Zh. Eksp. Teor. Fiz. **91**, 1897 (1986) [Sov. Phys. JETP **64**, 1124 (1986)].
[47] M.I. Dyakonov and F.G. Pikus, Solid State Commun. **83**, 413 (1992).
[48] B.J. van Wees, E.M.M. Willems, L.P. Kouwenhoven, C.J.P.M. Harmans, J.G. Williamson, C.T. Foxon, and J.J. Harris, Phys. Rev. B **39**, 8066 (1989).
[49] S. Komiyama, H. Hirai, S. Sasa, and S. Hiyamizu, Phys. Rev. B **40**, 12 566 (1989).
[50] G. Müller, D. Weiss, S. Koch, K. von Klitzing, H. Nickel, W. Schlapp, and R. Lösch, Phys. Rev. B **42**, 7633 (1990).
[51] A.H. MacDonald, T.M. Rice, and W.F. Brinkman, Phys. Rev. B **28**, 3648 (1983).
[52] V.T. Dolgopolov, S.I. Dorozhkin, and A.A. Shashkin, Zh. Eksp. Teor. Fiz. **92**, 1782 (1987) [Sov. Phys. JETP **65**, 999 (1987)].
[53] H.P. Wei, D.C. Paalanen, and A.M.M. Pruisken, Phys. Rev. Lett. **61**, 1294 (1988).
[54] H.P. Wei, S.Y. Lin, D.C. Tsui, and A.M.M. Pruisken, Phys. Rev. B **45**, 3926 (1992).
[55] S. Koch, R.J. Haug, K. von Klitzing, and K. Ploog, Phys. Rev. B **43**, 6828 (1991).
[56] S. Koch, R.J. Haug, K. von Klitzing, and K. Ploog, Phys. Rev. B **46**, 1596 (1992).
[57] V.T. Dolgopolov, A.A. Shashkin, B.K. Medvedev, and V.G. Mokerov, Zh. Eksp. Teor. Fiz. **99**, 201 (1991) [Sov. Phys. JETP **72**, 113 (1991)].
[58] M. D'Iorio, V.M. Pudalov, and S.G. Semenchinsky, in *High Magnetic Fields in Semiconductor Physics*, edited by G. Landwehr (Springer, New York, 1992), p. 56.
[59] H. Aoki and T. Ando, Phys. Rev. Lett. **54**, 831 (1985).
[60] A.M.M. Pruisken, Phys. Rev. Lett. **61**, 1297 (1988).
[61] B. Huckestein and B. Kramer, Phys. Rev. Lett. **64**, 1437

(1990).
[62] T. Ando, J. Phys. Soc. Jpn. **61**, 415 (1992).
[63] Y. Huo and R.N. Bhatt, Phys. Rev. Lett. **68**, 1375 (1992).
[64] T. Ando, A.B. Fowler, and F. Stern, Rev. Mod. Phys. **54**, 437 (1982).
[65] M.Ya. Azbel, Phys. Rev. B **45**, 4208 (1992).
[66] E. Abrahams, P.W. Anderson, D.C. Licciardello, and T.V. Ramakrishnan, Phys. Rev. Lett. **42**, 673 (1979).